tRNA as stabilizing matrix for fluorescent silver clusters: photophysical properties and IR study.

Tomash S. Sych[*a], Alexander M. Polyanichko [a], Ruslan R. Ramazanov [a] and Alexei I. Kononov [a]

[a]Saint Petersburg State University, Saint-Petersburg 199034, Russia

*email: inxalid@gmail.com

ABSTRACT

In this experimental study fluorescent silver clusters on tRNA matrix were synthesized for the first time. Obtained complexes have two emission regions in visible part of spectrum. We have also studied our complexes using FTIR spectroscopy. The possible binding sites of the clusters have been suggested.

Introduction

Studying the photophysical properties of the complexes between metal clusters and nucleic acids (NA), especially DNA, and proteins as a stabilizing matrix has been an important task for the last decade[1]. A great number of studies is currently devoted to the synthesis of luminescent silver (Ag) clusters on DNA of various nucleotide sequences[2,3]. It has been shown that the optical properties of the clusters strongly depend on the nucleotide sequence of the stabilizing matrix. It was suggested, that the clusters had elongated structure[4,5] and stabilized by two NA strands in the double-stranded regions[6–9]. Indeed, thread-like chains of Ag ions/atoms have been observed in some Ag-DNA crystal structures [10,11]. Currently, it has been accumulated a wealth of experimental material regarding synthesis of luminescent silver clusters on DNA. However, very little is known about the spectral properties and stability of the luminescent clusters on RNA[12,13]. In particular, transfer RNA (tRNA) has never been considered as such a stabilizing matrix before. Nowadays, approaches based on application of tRNAs labeled with various dyes are widely used[14–16]. However, they demonstrate limited applicability for intracellular imaging due to the high toxicity of the dyes. To overcome this limitation, we suggest to use tRNA as a stabilizing matrix for luminescent Ag clusters. tRNA has a specific secondary structure (Fig. 1)[17], with several loops and double helical regions[18,19], suitable for the cluster growing. Assuming that the formation of the stable luminescent nanoclusters on tRNA (tRNA-AgNCs) does not affect the native structure of tRNA (in particular, the CCA tail and the anticodon loop, which are essential for interactions with amino acids and mRNA respectively), it might allow one to apply this type of fluorophore for effective intracellular visualization of the different tRNA-associated processes in the living cell. We have synthesized two types of the clusters, emitting in green and red spectral regions. Using FTIR spectroscopy we have also analyzed structural changes in tRNA upon binding Ag ions and Ag clusters.

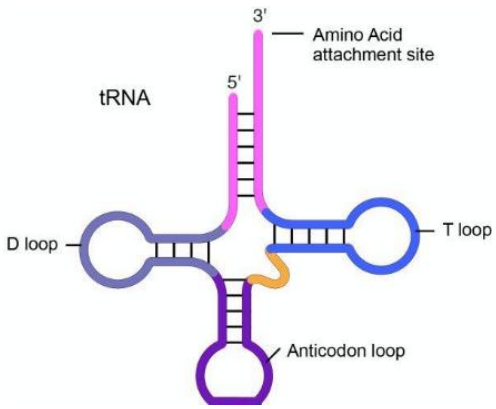

Figure 1. Secondary structure of tRNA.

Materials and Methods

Chemicals

Mixture of 20 natural tRNAs from E.Coli (Sigma-Aldrich #R1753, type XX), silver nitrate (AgNO3), sodium borohydride (NaBH4) and potassium bromide (KBr) were purchased from Sigma. Rhodamine 6G (R6G) was supplied by Lambda Physik.

Synthesis of fluorescent clusters

0.1 M AgNO3 solution was added to 0.24 mMPh (in moles of nucleotide) tRNA solution. The mixture was incubated for 1 hour under vigorous stirring at room temperature. Next, freshly prepared 1 mM NaBH4 solution was added into mixture. The final solution was kept at room temperature for 1 hour, after that was kept at 4°C in the dark until further analysis (usually at least 1 day). The optimal molar ratios (see "Results and Discussion") were as follows: [tRNA]:[Ag^+] = 2:1 and [Ag^+]:[NaBH4] = 2:1 for "green" type NCs; [tRNA]:[Ag^+] = 1:1 and [Ag+]:[NaBH4] = 4:1 for "red" type.

Spectral Methods

Fluorescence emission and excitation spectra were obtained at room temperature using a RF-6000 spectrofluorophotometer (Shimadzu). Fluorescence decay curves were obtained using a Fluorolog-3 spectrofluorometer (Horiba Jobin Yvon). The measurements were performed in a 0.4 cm quartz cuvette (Hellma Analytics). Long-wave pass filters were used to remove scattered light. The fluorescence emission spectra were corrected for instrument sensitivity. The fluorescence excitation spectra were corrected for the inner filter effect due to the high absorbance of the samples in the UV range as described elsewhere6. The bandpass for excitation and emission was set at 5 nm. Fluorescence lifetime measurements were performed with LEDs with full width half maximum (FWHM) of about 2 ns. Emission bandpass was set at 14 nm. The fluorescence quantum yield of the tRNA-AgNCs was measured using R6G in ethanol (QY = 0.95) as a reference[20]. Absorption spectra were obtained with a Specord 210 Plus double-beam spectrophotometer (Analytik Jena).

Prior to FTIR measurements all sample solutions were lyophilized using freeze drier Scientz-N12 (Vilitek). The obtained powder was used to prepare KBr pellets of each sample. IR spectra of the pellets were recorded using FTIR spectrometer Tensor 27 (Bruker), purged with dry nitrogen and equipped with MCT detector. Each spectrum was recorded with 4 cm-1 resolution and averaged by 128 accumulations. Background subtraction and baseline correction were performed using OPUS software provided by the spectrometer manufacture. Each spectrum was further normalized to obtain equal absorbance at 965 cm-1 attributed to a sugar ring vibration.

Results and discussion

To our best knowledge tRNA has never been used for NC synthesis before. Thus, first of all, we have determined the optimal conditions of the synthesis, based on the protocol, earlier developed for DNA oligonucleotides[7]. Obtained results demonstrated that in the case of tRNA there are two bands in green and red regions of the emission spectrum (Fig. 2). For further convenience, we will denote them as "green" and "red" types of NCs. In order to determine the optimal synthetic conditions for each type of the NCs the effects of pH and reaction time on their photophysical properties were studied.

Figure 3 shows the dependence of emission intensity on pH. In case of protonated tRNA (pH 5) rather weak emission was observed for both types of the clusters. Deprotonation of the tRNA (pH 10) slightly

improved the situation. However the maximal emission intensity was achieved at pH 7, which appears to be optimal for the synthesis of the both types of the clusters.

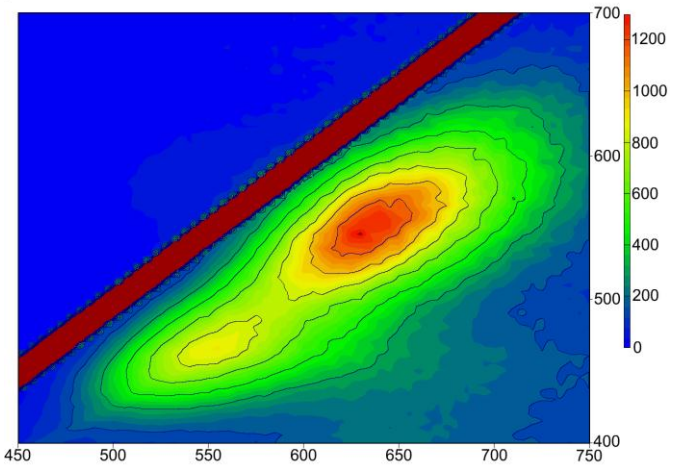

Figure 2. 2D fluorescence contour plot for tRNA-AgNCs.

We have also determined optimal proportions of the reagents required to obtain each type of the NCs (Table S1). Noteworthy, the type of the NCs dominating in the resulting complex depends on the ratio between Ag^+ ions and the reducing agent in the reaction mixture. Particularly, silver ions in excess of Ag^+ and of reducing agent form “green” NCs, while the lack of $NaBH_4$ resulted in formation of the “red” NCs. Most likely, the “red” clusters are larger and their self-assembling requires considerably longer period of time. It is also essential to note, that following either synthetic strategy we obtained both types of the clusters.

Figure 4 shows the spectral properties of the “red” clusters. For this type of the cluster one can observe narrow excitation and emission bands with a relatively small Stokes shift (0.3 eV). Figure 5 shows the spectral properties of the “green” clusters. It is interesting to note that the excitation maximum of the “red” cluster coincides with that of the “green” one (Fig. 5).

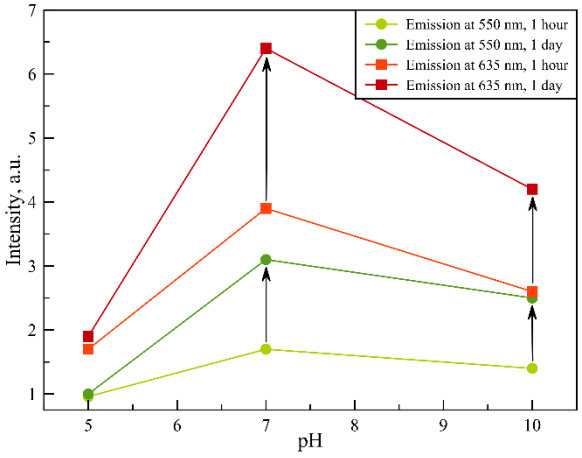

Figure 3. Emission intensity at 550 nm (two bottom curves) and 635 nm (two upper curves) with excitation at 280 nm.

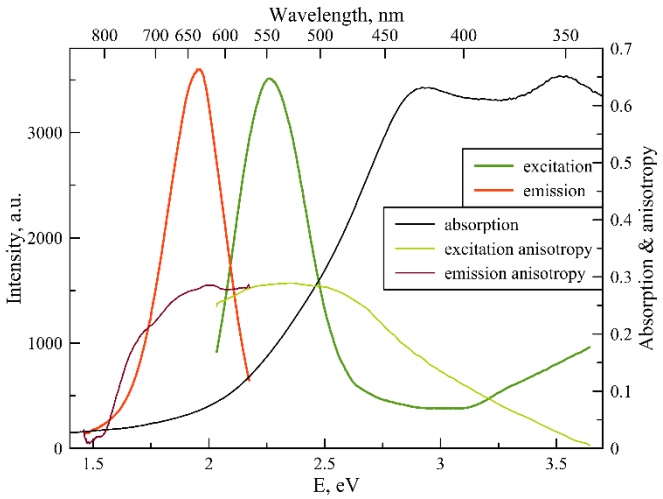

Figure 4. Fluorescence excitation, emission, excitation and emission anisotropy and absorption spectrum for "red" type of tRNA-AgNCs (λ_{ex} 550 nm, λ_{em} 635 nm).

We can note that the shape of the absorption spectrum is quite different from the shape of the excitation spectrum. It might indicate that we have rather heterogeneous system containing dark non-luminescent clusters and/or some large particles. The emission anisotropy curves of both clusters (Figs. 4, 5) exhibit quite typical behavior at the red slopes of the bands, that can be attributed to relaxation processes of nanosecond time scale and reorientation of the dipole moments of the emitters[21]. Multi-exponential behavior of the fluorescence decay curves (Figs. S3, S4) also might be considered as a manifestation of the relaxation[21].

Table 1. Photophysical properties and optimal reagent ratios for tRNA-AgNCs complexes

Cluster type		"green"	"red"
Reagent ratios	tRNA	equal	
	[tRNA]/[$AgNO_3$]	2:1	1:1
	[$AgNO_3$]/[$NaBH_4$]	2:1	4:1
Excitation maximum, nm		465	550
Emission maximum, nm		550	635
Stokes shift, eV		0.4	0.3
Lifetime, ns		0.7 (80 %) 2.7 (20 %) av. 1.1	1.4 (57 %) 3.1 (43 %) av. 2.1
Quantum yield		2 %	6 %

The major photophysical characteristics of the NCs are summarized in Table 1. The photophysical features (Stokes shifts, fluorescence decays, fluorescence anisotropy curves) of the clusters on tRNA resemble the properties of the clusters on DNA sequences[2,3], which likely indicates similar structural properties. We have obtained the FTIR spectra of pure tRNA and its complexes with Ag^+ ions and Ag clusters. The baseline corrected spectra in the range of 1900-800 cm^{-1} are presented in the Figure 6. The

mid-IR spectra of tRNA contain two major regions corresponding to the vibrations of the nitrogenous bases (1800 – ca. 1300 cm^{-1}) and to the vibrations of the sugar phosphate backbone (ca. 1300 - 800 cm^{-1}). A sharp band at 1384 cm^{-1} dominating in the spectra of the complexes is typical for the stretching vibrations of nitrates, which come from $AgNO_3$ used to prepare the complexes. Besides, some other features induced in RNA spectra by Ag^+ ions and silver nanoclusters can be noticed, which we summarized in the Table 2. The major assignments are based on the earlier published data regarding vibrational spectra of nucleic acids in general , and RNA in particular[22–27], and their complexes with silver ions[28–30].

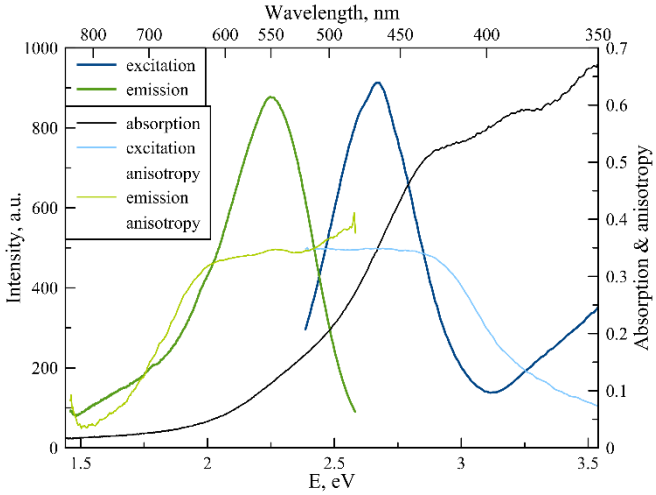

Figure 5. Fluorescence excitation, emission, excitation and emission anisotropy and absorption spectrum for “green” type of tRNA-AgNCs (λ_{ex} 465 nm, λ_{em} 550 nm).

In presence of Ag^+ ions distinct changes are observed in the spectra of the tRNA in both regions, mentioned above, attributed to the vibrations of the nitrogenous bases and the sugar phosphate backbone. Comparison of the absorption spectra of pure tRNA and the spectra of the complexes reveals the appreciable changes in vibrations at 1690 and 1576 cm-1. The former might be due to the guanine (G) C=O stretching and NH2 scissoring vibrations and/or interaction of the bases in the pairs[24], while the latter is typical for the interactions with N7 atom of guanine[22,23,27]. Also the changes in vibrational modes of cytosine can be clearly seen at 1650, 1604, 1530 and 1490 cm^{-1}. Vibrations at 1650 and 1604 cm^{-1} are attributed to the cytosine (C) in-plane ring vibrations, while the others at 1530 and 1490 cm^{-1} are involve NH and CH in-plane deformation modes of cytosine ring[24]. It is also worth mentioning that most of the above spectral features, as well as some less distinct changes observed in the spectra (see the Table 2) are characteristic for the base paring[23,27].

The major changes in vibrations of the sugar phosphate backbone at 1240, 1114, 1084, 1070, 937, 880, 870 and 814 cm-1 indicate that binding of the silver ions to tRNA resulting in considerable changes of the backbone geometry[24,25,31]. Most likely, the observed spectral pattern demonstrates that Ag+ ions primarily interact with GC pairs, resulting in their destabilization and, as a result, in destabilization of the double helical structure of tRNA. This conclusion agrees with the hyperchromic effect observed in the UV spectrum of tRNA upon binding with Ag+ ions (Fig. S5). The situation is remarkably different in case of tRNA complexes with silver nanoclusters. In the region of nitrogenous base vibrations the most considerable changes are observed in cytosine vibrations at 1650 cm-1, accompanied by slight intensity increase at 1690 and 1604 cm-1, both of which also involve cytosine ring vibrations.

Table 2. The Assignment of the Major Vibrations in the FTIR spectra. Bands marked with (+) and (-) in the complexes demonstrate respectively increase and decrease in absorbance compared to pure tRNA

Assignment (based on the data published elsewhere[22–31])	**Band position, cm^{-1}**		
	tRNA	tRNA-Ag^{+}	tRNA-AgNCs
Guanine C=O stretching coupled with NH_2 scissoring	1690	1683 (-)	1686 (+)
Cytosine in-plane ring vibration	1650 1604	1650 (+) 1607 (-)	1650 (+) 1603 (+)
Guanine C=N stretching	1576 sh	1576 sh	1576 sh
Cytosine NH and CH in-plane deformation modes of the ring	1529 1490	1531 (-) 1490 (-)	1530 (+) 1489 (+)
Antisymmetric phosphate stretching	1240	1238	1239 (+)
Ribose stretching at C2’	1114	1114	1114
Symmetric phosphate stretching	1084	1087 (+)	1087 (+)
-C-O-P- stretching in RNA	1062	1071 (+)	1071 (+)
Ribose –C-O-C- symmetric stretching	996 965	999 967	998 (-) 965 (+)
-C-O-P- stretching in RNA	937	937 (+)	938 (+)
Ribose ring –C-C- stretching	914	914 (-)	914 (-)
Ribose CH_2 rocking	879 867	881 870 (-)	880 (+) 869 (+)
Symmetric ribose stretching at C2’	812	814 (-)	816 (+)

Absorbance of the groups within the sugar phosphate backbone does not demonstrate considerable changes except for the bands at 1070, 937 cm^{-1}, also accompanied by slight changes in vibrations at 870 and 814 cm^{-1}. All of these bands are characteristic for RNA molecules[24,25,31], and noteworthy they demonstrate changes in the direction, opposite to those for tRNA-Ag^{+} complexes. Thus, we may conclude, that the binding of the silver clusters to the cytosine bases results in partial stabilization of the helical regions of the tRNA. We suggest, that upon reducing Ag+ ions, most of Ag atoms are released from RNA strands, and allowing tRNA to return to its native conformation. Remaining silver ions/atoms then assemble into the clusters stabilized by cytosine-rich regions in double-stranded RNA regions.

We can also notice here, that the complexes obtained have photophysical properties and binding sites similar to those typical for the clusters on DNA matrices. In case of short cytosine-rich DNA oligonucleotides[7], several types of luminescent clusters have been reported, including ones emitting in green (λ_{ex} 330 nm / λ_{em} 510 nm) and red (λ_{ex} 530 nm / λ_{em} 620 nm) spectral regions. It was also reported, that the clusters were stabilized by cysteine and thymine bases, which is in perfect agreement with our results, based on the analysis of the IR spectra of the complexes. Petty and co-authors used longer oligonucleotides, also enriched in cytosine with adenine inclusions[8]. As a result, they obtained green cluster (λ_{ex} 440 nm / λ_{em} 540 nm). In addition, it has been shown[32] that guanine-rich complementary sequence can activate the luminescence of the silver clusters. Hence, we can conclude that the mechanism of the formation and binding of luminescent silver clusters is likely similar for different NA sequences, regardless of the specific structure of the matrix. However, using molecules with particular biological functions as stabilizing matrices might greatly improve their applicability as biolabels.

Conclusions

We have showed that tRNA can stabilize fluorescent silver clusters. We have demonstrated the possibility to obtain complexes emitting in green (550 nm) and red (635 nm) regions of visible spectrum. FTIR study allowed us to identify possible binding sites for clusters, which appeared to be within the helical regions of tRNA. We have also shown that tRNA retained its double helical structure after the cluster formation. This strongly suggests that tRNA molecules in complex with NCs also retained their biological functions, which makes it possible to use them as a new class of intracellular biolabeling agents. We hope that the results obtained in this work will contribute in further development of fluorescent Ag-RNA complexes and their application for biological imaging.

Acknowledgements

This work was supported by the Russian Foundation for Basic Research (projects 18-33-00603 (cluster synthesis and photophysical studies) and 18-08-01500 (FTIR studies)) and by the Russian Science Foundation (project 17-73-10070 (tRNA assembly in the presence of silver ions)). Part of the spectral measurements were performed using equipment of Centre for Optical and Laser Materials Research Centre of Saint-Petersburg State University.

Notes and references

1 I. Chakraborty and T. Pradeep, Chem. Rev., 2017, 117, 8208–8271.

2 Z. Yuan, Y.-C. Chen, H.-W. Li and H.-T. Chang, Chem. Commun., 2014, 50, 9800–9815.

3 E. Gwinn, D. Schultz, S. M. Copp and S. Swasey, Nanomaterials, 2015, 5, 180–207.

4 D. Schultz, K. Gardner, S. S. R. Oemrawsingh, N. Markešević, K. Olsson, M. Debord, D. Bouwmeester and E. Gwinn, Adv. Mater., 2013, 25, 2797–2803.

5 R. R. Ramazanov and A. I. Kononov, J. Phys. Chem. C, 2013, 117, 18681–18687.

6 I. L. Volkov, Z. V. Reveguk, P. Y. Serdobintsev, R. R. Ramazanov and A. I. Kononov, Nucleic Acids Res., 2018, 46, 3543–3551.

7 R. R. Ramazanov, T. S. Sych, Z. V. Reveguk, D. A. Maksimov, A. A. Vdovichev and A. I. Kononov, J. Phys. Chem. Lett., 2016, 7, 3560–3566.

8 J. T. Petty, M. Ganguly, I. J. Rankine, E. J. Baucum, M. J. Gillan, L. E. Eddy, J. C. Léon and J. Müller, J. Phys. Chem. C, 2018, 122, 4670–4680.

9 S. M. Swasey, N. Karimova, C. M. Aikens, D. E. Schultz, A. J. Simon and E. G. Gwinn, ACS Nano, 2014, 8, 6883–6892.

10 J. Kondo, Y. Tada, T. Dairaku, Y. Hattori, H. Saneyoshi, A. Ono and Y. Tanaka, Nat Chem, 2017, 9, 956–960.

11 D. J. E. Huard, A. Demissie, D. Kim, D. Lewis, R. M. Dickson, J. T. Petty and R. L. Lieberman, J. Am. Chem. Soc.

12 K. A. Afonin, D. Schultz, L. Jaeger, E. Gwinn and B. A. Shapiro, Methods Mol. Biol., 2015, 1297, 59–66.

13 D. Schultz and E. Gwinn, Chem. Commun., 2011, 47, 4715–4717.

14 S. C. Blanchard, H. D. Kim, R. L. Gonzalez, J. D. Puglisi and S. Chu, PNAS, 2004, 101, 12893–12898.

15 S. C. Blanchard, R. L. Gonzalez, H. D. Kim, S. Chu and J. D. Puglisi, Nat. Struct. Mol. Biol., 2004, 11, 1008–1014.

16 I. L. Volkov, M. Lindén, J. A. Rivera, K.-W. Ieong, M. Metelev, J. Elf and M. Johansson, Nat. Chem. Biol., 2018, 14, 618.

17 H. Lodish, A. Berk, S. L. Zipursky, P. Matsudaira, D. Baltimore and J. Darnell, Molecular Cell Biology, W. H. Freeman, 4th edn., 2000.

18 R. W. Holley, J. Apgar, G. A. Everett, J. T. Madison, M. Marquisee, S. H. Merrill, J. R. Penswick and A. Zamir, Science, 1965, 147, 1462–1465.

19 J. L. Sussman, S. R. Holbrook, R. W. Warrant, G. M. Church and S. H. Kim, J. Mol. Biol., 1978, 123, 607–630.

20 R. F. Kubin and A. N. Fletcher, J. Lumin., 1982, 27, 455–462.

21 C. Cerretani, M. R. Carro-Temboury, S. Krause, S. A. Bogh and T. Vosch, Chem. Commun., 2017, 53, 12556–12559.

22 H. Fritzsche and C. Zimmer, Eur. J. Biochem., 1968, 5, 42–44.

23 M. Tsuboi, K. Shuto and S. Higuchi, Bull. Chem. Soc. Jpn., 1968, 41, 1821–1829.

24 M. Tsuboi, Appl. Spectrosc. Rev., 1970, 3, 45–90.

25 M. C. Chen and G. J. Thomas Jr., Biopolymers, 1974, 13, 615–626.

26 S. Alex and P. Dupuis, Inorg. Chim. Acta, 1989, 157, 271–281.

27 E. Taillandier and J. Liquier, Meth. Enzymol., 1992, 211, 307–335.

28 K. A. Hartman, Biochim. Biophys. Acta, Nucleic Acids Protein Synth., 1967, 138, 192–195.

29 D. E. DiRico, P. B. Keller and K. A. Hartman, Nucleic Acids Res., 1985, 13, 251–260.

30 H. Arakawa, J. F. Neault and H. A. Tajmir-Riahi, Biophys. J., 2001, 81, 1580–1587.

31 T. Sato, Y. Kyogoku, S. Higuchi, Y. Mitsui, Y. Iitaka, M. Tsuboi and K. Miura, J. Mol. Biol., 1966, 16, 180-IN4.

32 H.-C. Yeh, J. Sharma, J. J. Han, J. S. Martinez and J. H. Werner, Nano Lett., 2010, 10, 3106–3110.